Available online at www.sciencedirect.com
SCIENCE DIRECT®
Journal of Power Sources 129 (2004) 270–274
JOURNAL OF POWER SOURCES
www.elsevier.com/locate/jpowsour

Electrochemical characteristics of a-Si thin film anode for Li-ion rechargeable batteries

Ki-Lyoung Lee [a], Ju-Young Jung [a], Seung-Won Lee [a], Hee-Soo Moon [a], Jong-Wan Park [a,b,*]

[a] *Division of Materials Science and Engineering, Hanyang University, 17 Haengdang-Dong, Seongdong-Gu, Seoul 133-791, South Korea*
[b] *Research Center for Energy Conversion and Storage, San 56-1, Shilim-Dong, Kwangak-Gu, Seoul 151-742, South Korea*

Received 23 September 2003; accepted 20 October 2003

Abstract

Deposition of an amorphous Si (a-Si) thin film anode was carried out by a radio-frequency (rf) magnetron sputtering. In order to avoid mechanical disintegration of the Si electrodes, the Si was deposited on two types of Cu foil: normal Cu foil and Cu foil with a rough surface. The surface of the Cu foil was roughened with sandpaper. The properties of Si film were observed by FESEM, Raman, XRD, AFM, CLSM and electrochemical performance was evaluated. It was believed that the rough foil helped the active Si material to maintain the electronic contact with the current collector during charging and discharging.

Keywords: Li-ion rechargeable battery; Anode; Silicon; Thin film; Micro battery

1. Introduction

Graphitized carbon has been commonly used as the negative electrode material for commercial Li-ion batteries. However, the graphitized carbon cannot meet the capacity requirement of batteries needed for portable electric devices due to its restricted theoretical capacity (LiC_6, 372 mAh/g) [1–3], and the capacity of commercial graphite electrode was improved to the level approaching its theoretical capacity.

In recent years, Li alloys, e.g. Li_xM (M = Sn, Si, Ge, Al, etc.) have been studied extensively. Li alloys have a high volumetric and gravimetric capacity due to their high lithium packing density and safe thermodynamic potentials compared to carbonaceous materials like graphite [4–6]. For instance, tin-based materials can alloy with Li to give a theoretical capacity 994 mAh/g ($Li_{4.4}Sn$) [7,8]. However, the large volume difference (up to four times larger for $Li_{4.4}Si$ compared to Si) between the lithiated and lithium-free host causes pulverization problems of the metal particles, thereby inducing losses of electrical contact between active material and current collector [4]. Si can react with lithium to form alloys with a high Li/Si ratio at elevated temperature, such as $Li_{12}Si_7$, $Li_{13}Si_4$, Li_7Si_3 and $Li_{22}Si_5$ [9,10]. In the case of $Li_{22}Si_5$, the theoretical capacity is 4200 mAh/g. This is the highest capacity for any of the Li alloys studied to date. However, Si undergoes a larger volume change than any other alloy material during Li insertion and extraction (volume expansion ratio: 4.12). Thus, its capacity fade on cycling is remarkably rapid. Many attempts have been made to improve the electrochemical performance and minimize the mechanical stress caused by the large volume change of Si-based alloy electrodes [11–14]. They have focused on reducing the particle size of the host material, using multi-phase materials or intermetallic compounds. Although these solutions are desirable, they still have problems related to irreversible capacity loss and cyclability. The advantages of the thin film electrode prepared by means of various deposition methods including CVD, sputtering and evaporation, have been reported by many bulk- and micro-battery research groups [15–18]. However, the electrochemical performance is much worse when the two-dimensional film is thick. The reasons why such problems occur are the increased diffusion length of Li, the increase of resistance and stress damage in the film. Thus, the adhesion improvement between film and substrate and the stress distribution by structural change have been investigated by some groups [16–18].

The motivation for our work was to verify the improved electrochemical performance of the amorphous Si (a-Si) thin film electrode fabricated by rf magnetron sputtering. We investigated the charge-discharge characteristics of a-Si thin film with a rough surface of current collector in an attempt to overcome the mechanical disintegration due to volume change during Li insertion/removal. Expanding the contact

* Corresponding author. Tel.: +82-2-2290-0386; fax: +82-2-2298-2850.
E-mail address: jwpark@hanyang.ac.kr (J.-W. Park).

0378-7753/$ – see front matter © 2003 Elsevier B.V. All rights reserved.
doi:10.1016/j.jpowsour.2003.10.013

area between the deposited film and substrate may help the active Si material to accommodate volume change without pulverizing.

2. Experimental

Si thin films were deposited by radio-frequency (rf) magnetron sputtering. The chamber was evacuated down to 4.0×10^{-6} Torr as a base pressure and a working pressure of 5 mTorr was maintained with Ar gas. With a constant power density of 1.5 W/cm^2, 1–2 μm thick Si thin films were deposited on Cu foils as a current collector (13 μm in foil thickness). The Cu foils were roughened with 15 μm-grain sandpaper.

The crystallinity of the samples was characterized by X-ray diffractometry (RINT 2000, RIGAKU) and Raman spectroscopy (T64000, ISA Jobin-Yvon). The Raman spectra were collected at room temperature using the microscope attachment of the Raman spectrometer equipped with a charge coupled device (CCD) detector. The 50X objective lens of the microscope was used to focus the laser beam on a small selected area (about 2 μm^2) of the sample surface, and the backscattered Raman signal was collected. The Raman spectra were excited by Ar^+ laser lines at 514.4 nm and the laser power was kept at about 2 mW on the sample. The surface morphology of the films was obtained by field emission scanning electron microscopy (JES 6340F, JEOL) and atomic force microscopy (AP0190, Auto-Probe CP Multitask Microscopy). The arithmetic mean roughness (R_a) was measured with a confocal laser scanning microscope (Micro Systems LSM 410, Carl Zeiss). The electrochemical measurements were conducted with a typical two-electrode cell. The cell was composed of a metal lithium foil as a counter electrode, 1 M $LiPF_6$ in a 1:1 (v/v) mixture of ethylene carbonate (EC) and dimethyl carbonate (DMC) as electrolyte. The cells were assembled in an Ar-filled glove box. Galvanostatic charge-discharge half-cell tests were performed with a cycle tester (WBCS 3000, WON A TECH) using a constant current of 100 μA/cm^2. The cell was conducted between the initial OCV and 0.01 V versus Li^+/Li, then between 0.01 and 1.0 V after the first cycle. To obtain the cyclic voltammogram, the scan rate was set at 0.01 mV/s in the same experimental system and voltage range.

3. Results and discussion

3.1. Characterization of Si thin film

The morphologies of the Si film deposited on the Cu foil were examined by FESEM. The SEM image in Fig. 1 shows a cross-sectional view of the Si film deposited on flat Cu foil. The thickness of the dense Si film was found to be approximately 1.5 μm, which is close to the film thickness measured by the profilometric method (Alpha-Step 500, TENCOR). The thickness of the Si layer for the electrochemical test was 0.5 μm. A capacity estimation due to the amount of Si deposited was calculated assuming a density of 2.33 for the Si thin film indicating dense film.

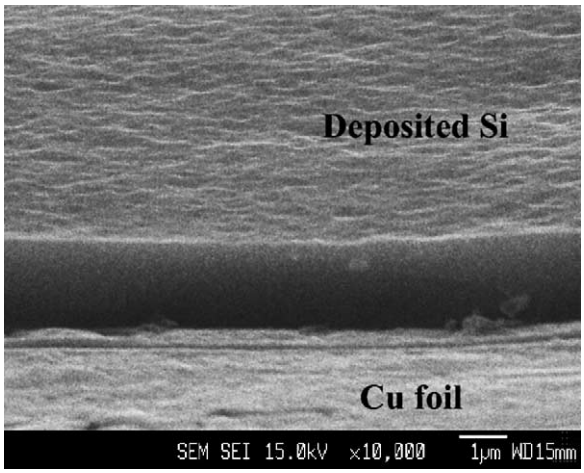

Fig. 1. Cross-section SEM image of Si thin film deposited on flat Cu foil.

Ex-situ Raman spectrum of the Si films is shown in Fig. 2. Deposited material was identified as an amorphous Si component because Raman spectroscopy detected the substantial presence of a peak around 480 cm^{-1} corresponding to an amorphous region and an absence of a peak around 520 cm^{-1} which characterizes a crystalline region [19]. Also, no diffractions except those of the Cu foil (JCPDS 03-1005) could be detected in the XRD patterns. (The data of XRD are not shown in this paper.) The amorphous structure of the electrode is usually more open compared with a well crystallized one. It has been recognized that a relatively open structure would adequately prevent the lattice expansion and have many Li diffusion paths. In general, the production of amorphous materials is well suited to thin films techniques such as rf sputtering or vacuum evaporation.

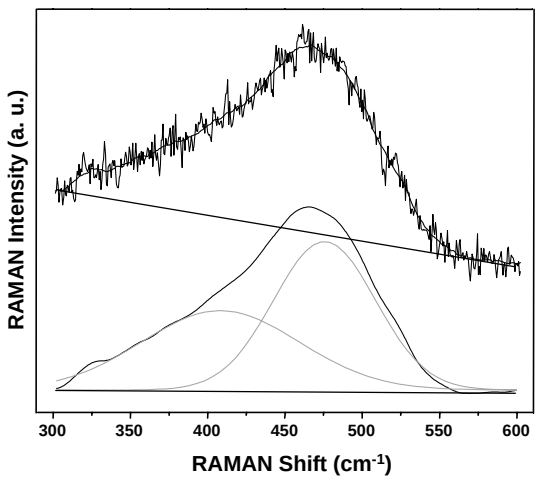

Fig. 2. Raman spectrum of Si thin film showing an amorphous component.

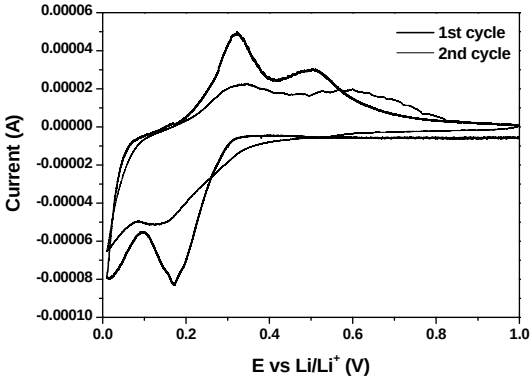

Fig. 3. The cyclic voltamogram of Si thin film.

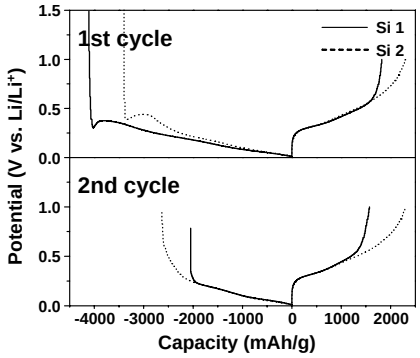

Fig. 5. Charge/discharge profiles of Si thin film deposited on Cu foils.

The Li insertion/removal into the film was done by CV (Fig. 3). From the CV results, it can be seen that Li insertion reaction occurred mostly at low potential below 0.2 V. The peaks obtained are attributed to the potential dependent formation and disappearance of Li-Si alloys of different compositions given by Wen and Huggins [9]. The difference in the potential for each peak can be ascribed to the kinetic effect involved in the CV measurement [18]. The peaks observed on the second cycle were compared with the first cycle in that two cathodic/anodic peaks decrease significantly at 0.2/0.3 V and an anodic peak at 0.5 V shifts toward a higher potential. The irreversible reaction of the first cycle seems to be associated with the formation of a solid electrolyte interface (SEI) layer or dangling bond which is related to phase transformation [11]. Therefore, the significant reduction of peak at 0.2 V indicated that the irreversible reaction was suppressed by maintaining the equilibrium state in the second cycle. The potential shift of about 0.1 V from 0.5 to 0.6 V also indicates increased kinetic polarization and internal resistance.

3.2. Charge and discharge characteristics with substrate

As shown in Fig. 4, there are morphological differences between the two Cu foils. Foil 1 had a relatively smooth surface, but foil 2 had a rough surface having corrugation and horizontal scratches. R_a was 0.101 μm for foil 1 and 0.256 μm for foil 2. High surface roughness means the large surface area of foil. The voltage-specific capacity profiles of the Si film deposited on the different two foils were performed by constant current charge/discharge measurements. Fig. 5 shows the 1st and 2nd charge/discharge curves of Si film measured between 0.01 and 1.0 V versus Li/Li^+ at a current density of 0.1 mA/cm^2. In the initial charge, the potential drops rapidly to 0.3 and 0.4 V, respectively and then gradually decreases to 0.01 V. This voltage fluctuation in the first charge may be due to the inactive properties of Si film against the electrochemical reaction. The Si anode on foil 1 (Si 1) having a higher charge capacity than that of foil 2 (Si 2) had a lower plateau caused by the hindrance of Li insertion. The first irreversible capacity losses of the two samples were about 32 and 56%, respectively. After the first cycle, the reversible charge-discharge reactions are maintained for the subsequent cycles. In the second charge, there is a distinct difference between Si 1 and Si 2. Si 1 drops rapidly to about 0.3 V as in the first charge, but Si 2 has smooth curve. This seems to indicate that the rough foil can help the Si electrode reduce polarization or internal resistance. From the discharge pattern in the second cycle, Si 2 exhibits stable cycle performance compared to Si 1. Their initial electrochemical characteristics of Si 1 and Si 2 are summarized in Table 1. $R_{10/1}$ was used to indicate a capacity retention upon repeated cycling. These results imply that adhesion was improved by increased contact area between Si film and the current collector.

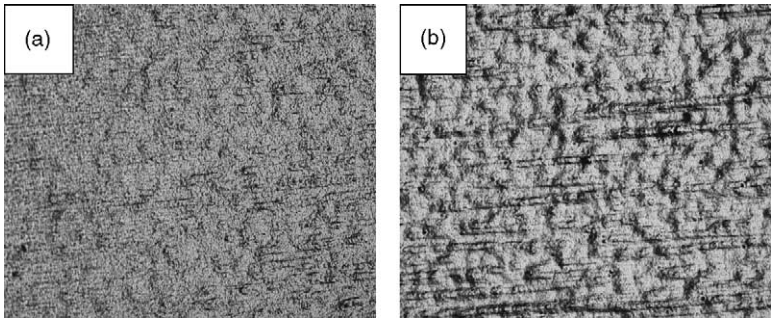

Fig. 4. Surface image of Cu foils: (a) foil 1 and (b) foil 2.

Table 1
Charge/discharge specific capacities in the first cycle

Cu foil (substrate)	Arithmetic mean roughness (μm)	Charge capacity (mAh/g)	Discharge capacity (mAh/g)	Coulomb efficiency (%)	$R_{10/1}$[a] (%)
Si 1	0.101	4120	1820	44.2	55.3
Si 2	0.256	3400	2300	67.6	79.4

[a] The ratio of the specific capacity in the 10th cycle relative to the first.

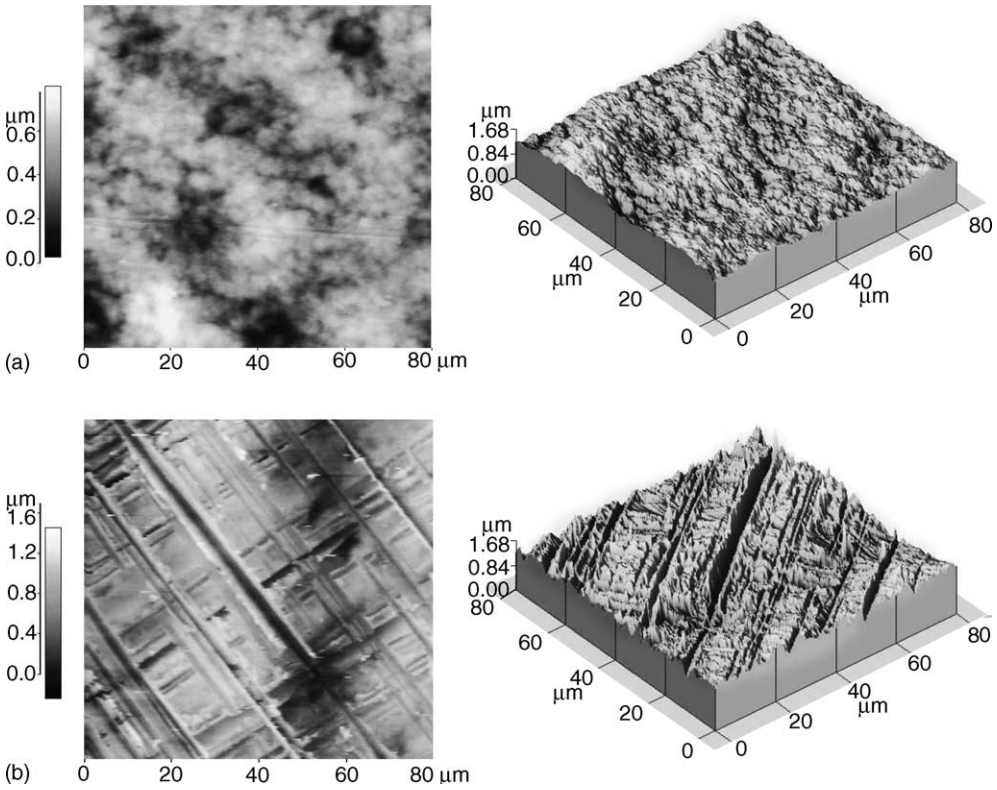

Fig. 6. AFM images of the surface of Cu foils: (a) flat foil (R_a: 0.101 μm) and (b) rough foil (R_a: 0.175 μm).

3.3. The effect of substrate grinding

AFM was used to examine the surface morphology of the two types of Cu foils (flat foil and roughened foil treated by grinding). Fig. 6 shows the two and three-dimensional AFM images of a 80 μm × 80 μm portion of flat and roughened foils. In Fig. 6b, it can be clearly seen that the surface is corrugated on the micrometer scale. This image shows that irregularities can be formed on a relatively flat surface (0.101 μm roughness) of Cu foil by grinding, increasing the surface roughness to 0.175 μm. This experiment is originated from the mechanical interlocking theory that the adhesion of the film was enhanced by increasing the contact area due to the roughened surface of the substrate [20]. Increasing the surface roughness (R_a) of a foil used as substrate improves the adhesion force between the foil and the active material. This adhesion enhancement reduces the effect of structural change, such as the crumbling or the falling-off of the active material that occurs when it expands or shrinks during storage or release of Li.

Fig. 7 shows the charge/discharge curve for the two types of Si electrodes in the first cycle. It was found that the difference of roughness and surface morphology between foils considerably affects the charge/discharge behavior, as can be

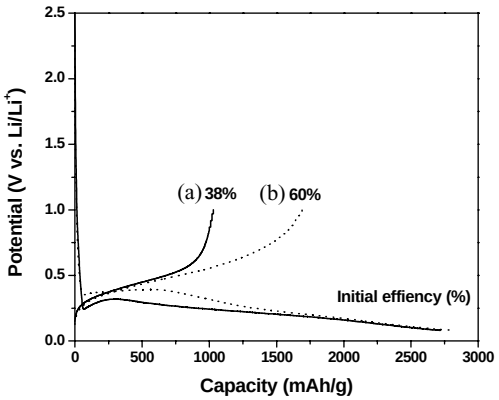

Fig. 7. The initial charge/discharge curves of Si thin film: (a) on flat Cu foil and (b) on rough Cu foil.

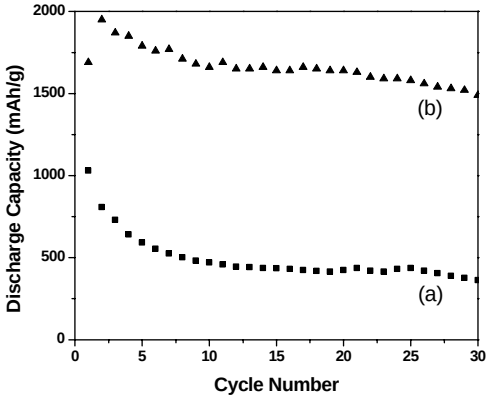

Fig. 8. The discharge capacity of a Si thin film: (a) on flat Cu foil and (b) on rough Cu foil.

seen in Fig. 5. There is a slight difference in the slope of the discharge curve. The discharge slope in the range 0.2–0.6 V of Si film on flat foil is steeper than that of the rough foil in the range 0.2–0.7 V. This subtle difference between slopes is attributed to electrochemical resistance induced in the first charge process. The roughened Cu foil treated by sand paper shows enhancement in initial coulombic efficiency and discharge capacity. The discharge capacity as a function of the number of cycles is shown in Fig. 8. Two samples were gradually degraded with cycling. However, the roughened foil showed an increase in discharge capacity compared to the flat foil. This indicates that controlling the surface properties of the foil is critical for obtaining a prolonged cycle life. Moreover, it is noted that the capacity of the second cycle slightly rises in the initial cycling stage. This result appears to be also linked to some kinetic factors. They may be gradual electrolyte penetration and more unimpeded Li transport into means going inside the electrode with repeated cycling.

4. Conclusions

Deposited film was identified as a-Si by Raman analysis. The Cu foil with a higher value of surface roughness, when used for the current collector, prevents a large voltage drop in charge/discharge profiles.

Si thin film on sanded Cu foil showed improved cyclability compared to untreated Cu foil. It was believed that expanding the contact area between the deposited film and the Cu foil helped the active Si material to accommodate a volume change.

Acknowledgements

This work was supported by KOSEF through the Research Center for Energy Conversion and Storage.

References

[1] S. Megahed, B. Scrosati, J. Power Sources 51 (1994) 79.
[2] T. Ohzuku, Y. Iwakoshi, K. Sawai, J. Electrochem. Soc. 140 (1993) 2490.
[3] D. Aurbach, Y. Ein-Eli, B. Markovsky, A. Zaban, S. Luski, Y. Carmeli, H. Yamin, J. Electrochem. Soc. 142 (1995) 2882.
[4] J.O. Besenhard, J. Yang, M. Winter, J. Power Sources 68 (1997) 87.
[5] V. Manev, I. Naidenov, B. Puresheva, G. Pistoia, J. Power Sources 57 (1995) 133.
[6] S. Kuwabata, N. Tsumura, S. Goda, C.R. Martin, H. Yoneyama, J. Electrochem. Soc. 145 (1998) 1415.
[7] J.O. Besenhard (Ed.), Handbook of Battery Materials, VCH, 1998.
[8] R.A. Huggins, Solid State Ionics 57 (1998) 113.
[9] C.J. Wen, R.A. Huggins, J. Solid State Chem. 37 (1976) 271.
[10] R.N. Seefurth, R.A. Sharma, J. Electrochem. Soc. 124 (1977) 1207.
[11] H. Li, X. Huang, L. Chen, Z. Wu, Y. Liang, Electrochem. Solid-State Lett. 2 (1999) 547.
[12] G.A. Roberts, E.J. Cairns, J.A. Reimer, J. Power Sources 110 (2002) 424.
[13] K. Il-Seok, P.N. Kumta, G.E. Blomgren, Electrochem. Solid-State Lett. 3 (2000) 493.
[14] J. Yang, Y. Takeda, N. Imanishi, C. Capiglia, J.Y. Xie, O. Yamamoto, Solid State Ionics 152–153 (2002) 125.
[15] A.M. Wilson, J.R. Dahn, J. Electrochem. Soc. 142 (1995) 326.
[16] S. Bourderau, T. Brousse, D.M. Schleich, J. Power Sources 81–82 (1999) 233.
[17] T. Yoshida, T. Fujihara, H. Fujimoto, R. Ohshita, M. Kamino, S. Fujitani, The 11th IMLB, Monterey, CA, USA, Abstract No. 48, 2002.
[18] S. Ohara, J. Suzuki, K. Sekine, T. Takamura, J. Power Sources 119–121 (2003) 591.
[19] T. Motooka, O.W. Holland, Appl. Phys. Lett. 58 (1991) 2360.
[20] A.J. Kinloch, J. Mater. Sci. 15 (1980) 2141.